INSTITUTE OF PHYSICS PUBLISHING JOURNAL OF MICROMECHANICS AND MICROENGINEERING

J. Micromech. Microeng. **15** (2005) S259–S267 doi:10.1088/0960-1317/15/10/S02

Micro manipulation by adhesion with two collaborating mobile micro robots

W Driesen[1], T Varidel[1], S Régnier[2] and J-M Breguet[2]

[1] Laboratoire de systèmes robotiques, Ecole Polytechnique Fédérale de Lausanne, EPFL-LSRO, Station 9, CH-1015 Lausanne, Switzerland
[2] Laboratoire de Robotique de Paris, Université Pierre & Marie Curie, UPMC-CNRS, BP 61 92265 Fontenay Aux Roses, France

E-mail: walter.driesen@epfl.ch

Received 14 January 2005, in final form 27 April 2005
Published 6 September 2005
Online at stacks.iop.org/JMM/15/S259

Abstract
A micro manipulation platform consisting of two cubic centimeter sized micro robots each with four degrees of freedom has been developed. This paper discusses four different strategies of manipulation by adhesion for grasping, transferring and releasing a micro object. For each strategy, the interacting forces have been modeled and the results are compared with the real behavior of $\varnothing 40\ \mu$m pollen micro spheres that are manipulated with the developed micro robots. Both theoretical model and experimental results show that the developed micro robots and the proposed strategies are well suited for the manipulation of the proposed micro objects.

M This article features online multimedia enhancements

(Some figures in this article are in colour only in the electronic version)

1. Introduction

In the last few decades, the fabrication of individual micro components has taken a large step forward through the development of new—mostly silicon based—fabrication technologies and the definition of industrial processes and standards. Micro assembly of several micro components into one micro system, however, is a step that is still very challenging and is a domain of intensive research nowadays.

Two different approaches can be adopted when developing a station for micro manipulation: the approach based on stationary robots and the approach based on small mobile robots. The advantage of a station based on stationary robots is that it is easier to integrate position feedback on all the degrees of freedom, which allows for high-precision motion and a high degree of automation. The advantage of a station based on mobile robots lies in the increased flexibility. The small dimensions, the degrees of freedom and the large working range of mobile robots allow us to work in confined spaces (for instance, a scanning electron microscope or a micro factory) and to rearrange the robots in the optimal position for a certain task. That is why a station based on small mobile robots finds its most interesting application in research in the field of micro manipulation and micro assembly and not in the field of industrial mass assembly of micro objects.

Sulzmann *et al* [1] developed a setup consisting of a micro robot of several cubic centimeters and vision feedback for micro assembly. Fatikow *et al* [2] present a micro assembly station based on cubic decimeter sized mobile micro robots for micro manipulation under an optical microscope or inside a scanning electron microscope. Martel *et al* [3] have conceived a mobile micro robot of some cubic centimeters equipped with an SPM probe for local measurements. Several other mobile micro robots have been developed [4, 5], but these robots have not yet been used as agents for a micro manipulation setup. The major drawbacks of the mobile micro robotic approach for micro manipulation are the difficulty of integrating the required sensors (e.g., position, force, etc) and the wires in the case of tethered robots or the powering and onboard electronics in the case of untethered robots.

In the MiCRoN project[3], the participating institutes try to go one step further by realizing a small cluster of untethered cooperating agents, each of them smaller than any piezoelectrically actuated robot before. The agents operate in a special environment, which comprises a power floor for energy

[3] More information is available at http://microrobotics.ira.uka.de.

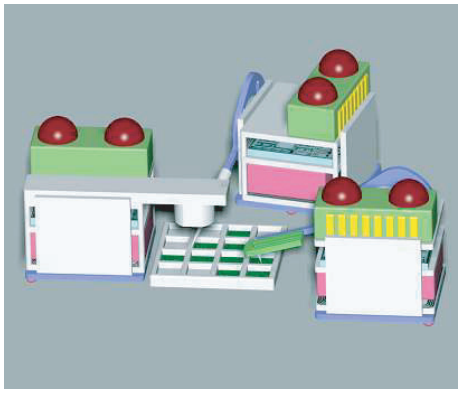

Figure 1. A possible scenario of cooperating robots with different tools (sensor, needle tool and injection chip).

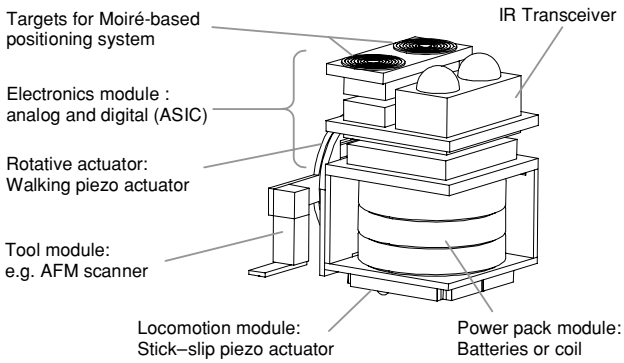

Figure 2. Structure of the untethered micro robot developed within the MiCRoN project ($12 \times 12 \times 17.5$ mm^3).

supply by inductive means and a smooth surface permitting a positioning with the required resolutions, as well as a global positioning system and a host computer communicating with the agents by IR transmission. The robots allow us to work with a resolution of some nanometers and with a high absolute precision of 5 μm in a workspace of more than 500×500 mm^2 [6]. Figure 1 shows a view of a possible scenario of microhandling with three cooperating robots, each with a different tool.

This paper discusses different handling experiments based on micro manipulation by adhesion that have been carried out with two tethered mobile micro robots developed within the MiCRoN project. The next section presents the micro robots that have been used for these experiments. In section 3 an introduction to surface forces at the micro-scale is given. Section 4 discusses different strategies for micro manipulation by adhesion. For each strategy the results of a theoretical model of the surface forces are compared to the real behavior observed in the experiments. The paper concludes with a summary of the most important results and conclusions.

2. Micro robotic platform

2.1. Wireless prototype

Figure 2 presents the cubic centimeter sized micro robot developed in the MiCRoN project. It consists of the following:

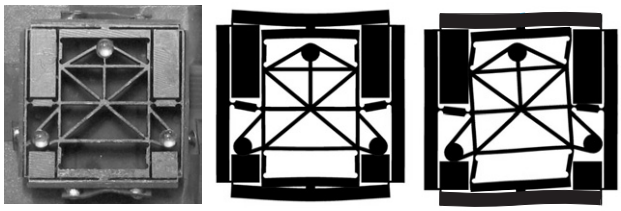

(*a*) Picture (*b*) Translation (*c*) Rotation

Figure 3. Locomotion module ($10 \times 10 \times 1$ mm^3) (*a*) based on the stick and slip principle with the working principle in translation (*b*) and rotation (*c*).

- onboard electronics module for low-level intelligence, information transmission, driving circuitry for sensors and actuators, IR transceiver;
- locomotion module based on piezoelectric actuators;
- power pack (battery and/or inductive transmission);
- tool module (different configurations).

Different modules can be used upon assembly of the robot in order to meet the requirements of certain applications. The power module, for instance, can either be a coil for energy transmission, or a battery for a short autonomous operation without the interference from a surrounding magnetic field. The tool modules carry micro tools such as a needle for micro manipulation, a micro gripper, a syringe chip for micro injection or a miniaturized scanning probe.

2.2. Tethered prototype

The electronics of the wireless robot presented in figure 2 is currently being assembled, so for the moment only tethered prototypes are used. In the tethered prototype, the electronics is replaced by a brass weight in order to increase the contact force of the robot and thus reducing the disturbing influences of the wires. The different degrees of freedom of the robot are provided by a locomotion platform (X, Y, θ_z) and a rotary arm actuator (θ_x) presented below.

2.2.1. The locomotion platform. The locomotion module [7] ($10 \times 10 \times 1$ mm^3) consists of a steel frame, in which a flexible structure is cut out by laser machining (figure 3(*a*)). Four piezoceramic bars are assembled to the frame on the sides and three sapphire half-spheres, serving as feet, are glued on top of the circular surfaces of the frame. The assembly of the piezoactuators on steel results in four heterogeneous bimorph actuators (also called 'monomorph' or 'unimorph' actuators), whose deformation is combined into XY-motion of the feet by the flexible steel frame (figure 3(*b*)). The electrodes of two of the four bending actuators are split in the middle. A rotational displacement of the platform is thus obtained by applying an opposite voltage to both electrode halves (figure 3(*c*)). A long-range motion is obtained for the three degrees of freedom by applying a sawtooth signal, resulting in a stick and slip motion of the robot [8]. Hence the locomotion platform provides the micro robot with three degrees of freedom (X, Y, θ_z) for three independent driving signals. The maximum velocity of this locomotion platform is about 0.35 mm s^{-1} with a sawtooth signal of 20 Vpp and 2500 Hz and more than 2 mm s^{-1} for 400 Vpp and 1500 Hz.

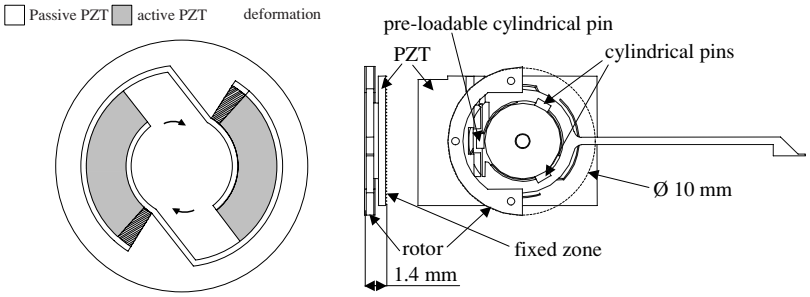

(*a*) (*b*)

Figure 4. A rotary actuator based on a PZT actuator and the stick and slip principle. (*a*) Principle of the rotary actuator for tool positioning. (*b*) Guiding system for rotary actuator.

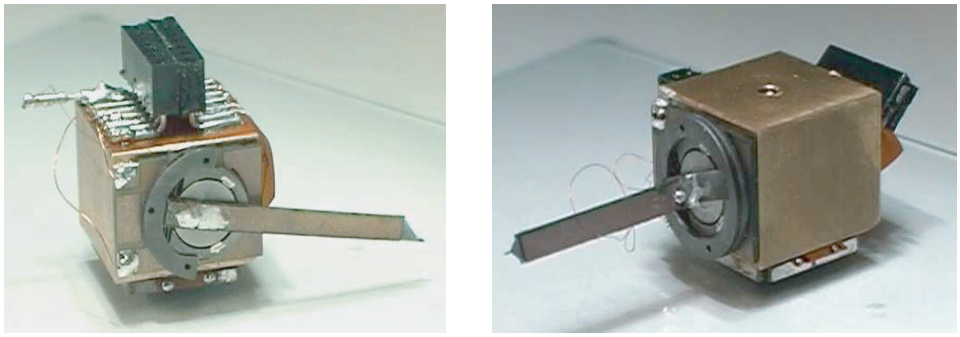

(*a*) (*b*)

Figure 5. Two 4 DOF mobile micro robots with a rotational arm ($12 \times 12 \times 12$ mm^3). (*a*) Arm in plane of rotation. (*b*) Arm perpendicular to plane of rotation.

Once the desired position is within the distance of one step length, the robot switches to the scanning mode and reaches its final position by applying a slowly varying dc voltage to the piezoelectric actuators. Repetitive steps of 7 nm back and forth have been realized with this locomotion platform. The combination of a stepping mode and a scanning mode within the same locomotion platform results in the unique combination of a long-range motion with a nanometric resolution [8].

2.2.2. A rotary actuator for tool positioning. For the positioning of the tools, a rotary micro actuator also based on the stick and slip principle has been developed [9]. The driving element of the stick and slip system is a piezoelectric plate of which two zones in the shape of the perimeter of a circle sector are liberated by some laser cuts and activated by electrode structuring. When excited with the same signal, these active zones expand, resulting in a small rotatory movement of the inner part (see figure 4(*a*)). A disc with a V-groove on its perimeter is glued on top of the rotating inner part. The rotor of the actuator is provided with three cylindrical pins that slide in this V-groove. One of these pins is fixed on a spring element in order to provide the required pre-load (figure 4(*b*)).

The single-layer piezoelectric actuator has to be driven with a sawtooth signal of at least 100 Vpp. The maximum velocity of 4 rpm is reached with a signal of 400 Vpp and 3 kHz and the maximum torque is 0.13 mN m. Both maximum velocity and maximum torque are more than sufficient for micro manipulation tasks. The great advantage of this actuator is the resolution of a few nanometers with an arm length of 19 mm when it is actuated in the scanning mode.

2.3. Micro manipulation setup

Two different versions of the micro robots described above have been used for the experiments described in this paper. In the first version the arm is assembled in the plane of rotation, resulting in a vertical motion of the tool (see figure 5(*a*)). In the second version the arm is assembled perpendicularly to the plane of rotation, resulting in a rotation of the arm around its own axis (figure 5(*b*)).

On both of the rotating arms another piezoelectric actuator is assembled on top of which a piece of silicon, serving as the tool for micro manipulation by adhesion, is glued. Hence, by applying a pulse to the piezoelectric actuator a high acceleration is transmitted to the silicon tool. As will be shown in section 4.4, this acceleration can be used for the release of the micro object sticking to the piece of silicon.

For the experiments, the two robots have been arranged as shown in figure 6. A microscope with a field of view of $170 \times 130\,\mu$m^2 generates a local view from the side and a microscope with a field of view of 4×3 mm^2 generates a more global view from the top. This setup consisting of two mobile robots each with four degrees of freedom without any severe limitations in range has a major advantage of great flexibility, which has been proven to be very useful during experiments presented in this paper.

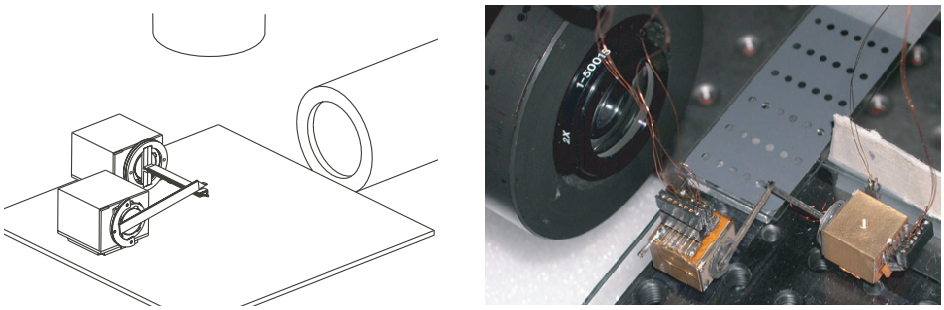

Figure 6. Setup for micro manipulation with two mobile micro robots and two microscopes (top view and side view).

3. Adhesion forces

The adhesion phenomena are mainly a result of intermolecular potentials, as expressed by Van der Waals forces. Capillarity and electrostatic are also environment-dependent forces that contribute to the adhesion. For micro-scale objects, these forces have higher magnitudes than the gravitational force and they are mainly attractive. Nevertheless, they depend on the inverse square or cube of the distance between the surfaces, for example, for Van der Waals, and their influence becomes obvious in contact. A minimum amount of force is thus necessary to separate two mediums in contact. This force is commonly called *pull-off*. In the case of a sphere (radius R) on a planar surface, its expression is approximately given by the JKR (for the lower boundary) or DMT (for the higher boundary) contact models [10, 11],

$$\tfrac{3}{2}\pi R W_{12} \leqslant A \leqslant 2\pi R W_{12} \tag{1}$$

where W_{12} is the work of adhesion between the two mediums. W_{12} is expressed as $W_{12} = \gamma_1 + \gamma_2 - \gamma_{12} = 2\sqrt{\gamma_1\gamma_2}$ with γ_{12} interfacial energy, and γ_1 and γ_2 surface energies of the object and the substrate or tool.

According to [12], the λ coefficient can be used to choose the most appropriate contact model for a given case. This coefficient is expressed for an interface between two bodies 1 and 2 with

$$\lambda_{12} = 2\sigma_0 \left(\frac{R}{\pi W_{12} K^2}\right)^{\frac{1}{3}} \tag{2}$$

with σ_0 chosen to match the minimum adhesive stress of a Lennard–Jones potential (with equilibrium separation z_0) [12] and K the equivalent elastic modulus:

$$K = \frac{4}{3}\left(\frac{1-\nu_1^2}{E_1} + \frac{1-\nu_2^2}{E_2}\right)^{-1} \tag{3}$$

Using λ, the pull-off force can be estimated with [13]:

$$\lambda < 0.1 \Rightarrow \text{DMT} \qquad A = 2\pi R W_{12} \tag{4}$$

$$0.1 < \lambda < 5 \Rightarrow \text{Dugdale}$$
$$A = \left(\frac{7}{4} - \frac{1}{4}\frac{4.04\lambda^{\frac{1}{4}} - 1}{4.04\lambda^{\frac{1}{4}} + 1}\right)\pi R W_{12} \tag{5}$$

$$\lambda > 5 \Rightarrow \text{JKR} \qquad A = \frac{3}{2}\pi R W_{12}. \tag{6}$$

The moment of maximum rolling resistance of a sphere on a planar surface is given by [14]

$$M_{\max} = c_r W_{12} a \tag{7}$$

Table 1. Adhesion-related material constants for the materials involved in the experiments presented in this paper.

		Silicon	Pollen	Teflon
Surface energy (mJ m^{-2})	γ	1400	35.5	18
Poisson's ratio	ν	0.17	0.39	0.46
Young's modulus (GPa)	E	140	3.4	0.5

where c_r is the maximum resistance coefficient, and a is the contact radius between the object and the substrate or tool. c_r has been estimated to be $c_r = 1 \times 10^{-5}$ m [15]. The contact radius a is expressed, for different values of λ, by

$$\lambda < 0.1 \Rightarrow \text{DMT} \quad a = \left(\frac{R}{K}(P + 2\pi R W_{12})\right)^{\frac{1}{3}} \tag{8}$$

$$0.1 < \lambda < 5 \Rightarrow \text{Dugdale} \quad a = a_0 \left(\frac{\alpha + \sqrt{1 + \frac{P}{A}}}{1+\alpha}\right)^{2/3} \tag{9}$$

$$\lambda > 5 \Rightarrow \text{JKR}$$
$$a = \left[\frac{R}{K}\left(P + 3\pi R W_{12} + \sqrt{6\pi R W_{12} P + (3\pi R W_{12})^2}\right)\right]^{\frac{1}{3}} \tag{10}$$

with P the component of the external load perpendicular to the surface and K the equivalent elastic modulus. a_0 is calculated with

$$a_0 = \left(1.54 + 0.279\frac{2.28\lambda^{\frac{1}{3}} - 1}{2.28\lambda^{\frac{1}{3}} + 1}\right)\left(\frac{\pi W_{12} R^2}{K}\right)^{\frac{1}{3}} \tag{11}$$

and α is obtained by $\lambda = -0.924\ln(1 - 1.02\alpha)$.

The micro objects handled in the experiments in this paper are pollen (ambrosia) micro spheres with an average diameter of about $\varnothing 40\,\mu$m. Table 1 presents the adhesion-related material constants for silicon, pollen and teflon. The maximum friction coefficient between pollen and silicon and between pollen and teflon is about 0.1.

For these material constants the λ coefficient is calculated as $\lambda_{\text{pollen,teflon}} = 39.03$ and $\lambda_{\text{pollen,silicon}} = 45.02$. So for both interfaces the JKR model will be used. The pull-off force of a $\varnothing 40\,\mu$m pollen micro sphere to a teflon substrate and a silicon tool can thus be calculated with equation (6)

$$A_{\text{pollen,teflon}} = 4.8\,\mu\text{N} \tag{12}$$
$$A_{\text{pollen,silicon}} = 42\,\mu\text{N}. \tag{13}$$

The weight G of such a sphere is only

$$G = 0.18\text{nN} \qquad \text{for} \quad \rho_{\text{pollen}} = 549\ \text{kg m}^{-3}. \tag{14}$$

Figure 7. Grasping of a pollen micro sphere adhering to a teflon substrate by approaching it with a silicon tool.
M An MPEG movie of this figure is available from stacks.iop.org/JMM/15/S259

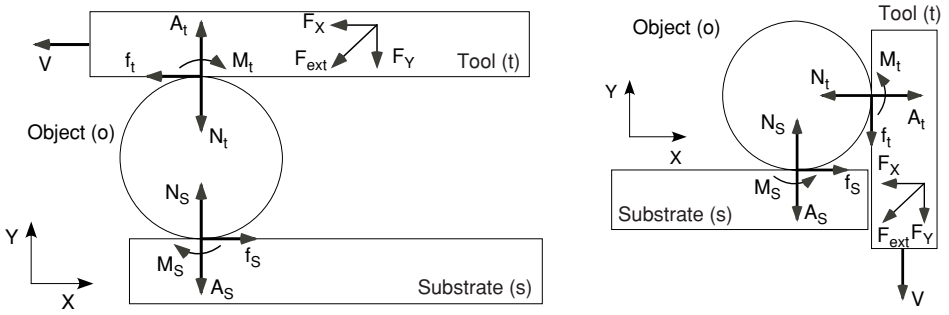

(*a*) Transfer by rolling (*b*) Transfer by scraping

Figure 8. The principle of transfer by rolling and scraping.

These results clearly show that the weight is negligible for the micro objects considered in this work. Gravity forces will be neglected from now on.

4. Strategies for micro manipulation by adhesion

Four different strategies for grasping, transferring and releasing a micro object or for transferring it from one tool to another tool have been studied. All these strategies have been experimentally realized with a setup consisting of the two 4 DOF micro robots from figure 5 and two microscopes, one giving a top view and the other giving a side view of the tools and the micro objects.

4.1. Grasping from a substrate with low adhesion

As the work of adhesion in equation (6) is strongly material dependent, the micro object can be transferred from a tool or substrate with a low surface energy to a tool or substrate with a high surface energy. Figure 7 shows the grasping of a pollen micro sphere adhering to a teflon substrate with the silicon tool fixed on the micro robot. This strategy is relatively simple to put into practice and has proven to be very reliable. However, as it is a transfer that only works in one direction—the direction of materials with increasing surface energy—other strategies are necessary for a useful manipulation sequence.

4.2. Transfer by rolling

In the second strategy, the micro object is transferred from the substrate to the tool by approaching it with the tool and rolling it over the corner of the substrate by moving the tool parallel to the substrate (figure 8(*a*)). A necessary condition for the successful transfer by rolling is that the micro object is effectively rolling between the tool and the substrate and not just sliding on the tool. The rest of this section presents a theoretical model to express this condition in equations and compares the results with the experimental results.

On the assumption of a quasistatic process and in the case of negligible gravity forces, the following equilibrium equations are obtained:

$$F_x = f_\mathrm{t} = f_\mathrm{s} \tag{15}$$

$$N_\mathrm{t} = A_\mathrm{t} + F_y \tag{16}$$

$$N_\mathrm{s} = A_\mathrm{s} + F_y \tag{17}$$

$$R(f_\mathrm{t} + f_\mathrm{s}) = M_\mathrm{t} + M_\mathrm{s}. \tag{18}$$

Sliding between the tool and the object occurs when the required friction force f_t at the tool interface exceeds its maximum value:

$$f_\mathrm{t} = F_x > f_\mathrm{t,max} = \mu N_\mathrm{t} \tag{19}$$

with equation (16) and (6)

$$F_x > \mu\left(\tfrac{3}{2}\pi W_\mathrm{t} R + F_y\right). \tag{20}$$

Rolling occurs when the moment generated by both friction forces exceeds the sum of the maximum rolling resistances at tool and substrate interfaces (see also (18)),

$$R(f_\mathrm{t} + f_\mathrm{s}) > M_\mathrm{t,max} + M_\mathrm{s,max} \tag{21}$$

With equation (15) and (7) the condition for rolling becomes

$$F_x > \frac{c_\mathrm{r}}{2R}(W_\mathrm{s} a_\mathrm{s} + W_\mathrm{t} a_\mathrm{t}) \tag{22}$$

in which a_s and a_t can be calculated from equation (10) for $P = F_y$.

Rolling occurs when the limit for rolling is reached earlier than the limit for sliding or with (20) and (22):

$$\frac{c_\mathrm{r}}{2R}(W_\mathrm{s} a_\mathrm{s} + W_\mathrm{t} a_\mathrm{t}) < \mu\left(\frac{3}{2}\pi W_\mathrm{t} R + F_y\right). \tag{23}$$

Solving this implicit equation results in a relation between F_y and R that gives for a certain object diameter D (or radius R)

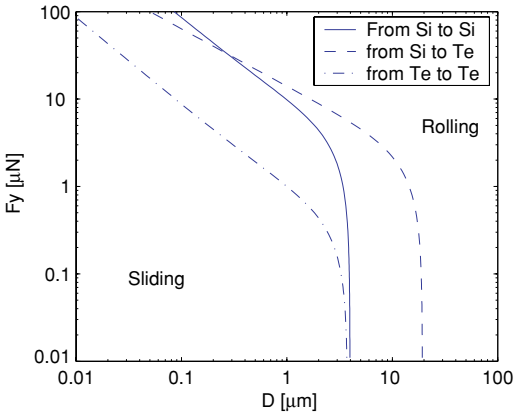

Figure 9. Conditions for rolling for the transfer by rolling strategy.

the minimum external load F_y that must be applied in order to force the object to roll. Figure 9 shows these rolling limits for the following three cases: transfer from a silicon substrate to a silicon tool, transfer from a silicon substrate to a teflon tool and transfer from a teflon substrate to a teflon tool. It can be seen that a rolling transfer in the case of equal materials is always possible, no matter which external contact force is applied, if the diameter of the object is larger than the critical diameter of $\varnothing 4\,\mu$m. For lower diameters the contact force has to be increased.

Equation (10) shows that the contact radius a is proportional to $R^{\frac{2}{3}}$ if the external load $P = 0$ (here $P = F_y$). Consequently, the left part of equation (23) scales with $R^{-\frac{1}{3}}$ while the right part is proportional to R. This explains why figure 9 shows that there is a certain critical diameter, below which the object will not roll, but slide. The fact that rolling of a small diameter object ($<4\,\mu$m) can be made possible by increasing the contact force can be explained by the fact that the sliding friction increases linearly with the external load, while the rolling resistance increases less than linearly with the external load as can be seen from equations (23) and (10).

At low contact forces, the rolling limit for the transfer from silicon to silicon seems to be equal to the rolling limit for the transfer from teflon to teflon. This is because at low external contact forces the rolling limit is proportional to $W\,(W/K)^{\frac{1}{3}}$ while the sliding limit is proportional to μW. The friction coefficient μ between silicon and pollen and between teflon and pollen is about the same. The work of adhesion W is about 10 times smaller in the case of teflon, and so is the equivalent elastic modulus K. Hence, for low contact forces, W/K is constant and so both rolling and sliding limits scale linearly with W, so the critical diameter does not change between a silicon–silicon transfer and a teflon–teflon transfer. However,

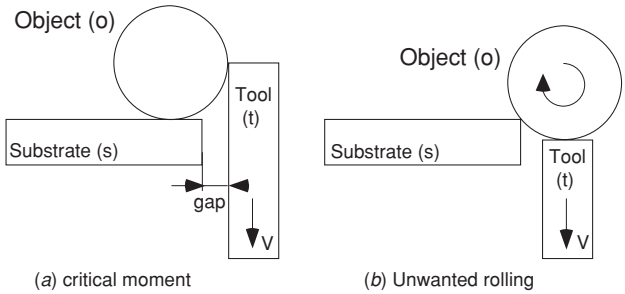

Figure 11. Possible behavior of an object during transfer by scraping.

in the case of teflon the external load $P = F_x$ starts to dominate in equation (10) at force values that are about 10 times smaller than in the case of silicon, which is confirmed by figure 9. Finally, it can also be concluded from the graph that a transfer from a silicon substrate to a teflon tool by rolling is more complicated as sliding will occur only at the teflon interface (i.e., low friction force), while rolling has to occur at both the teflon and the silicon interface (i.e., intermediate rolling resistance).

Figure 10 shows the transfer by the rolling strategy of a $\varnothing 40\,\mu$m sphere from the silicon tool of one robot to another. Rolling can be clearly distinguished from sliding as the translational velocity of the micro sphere in the case of rolling is half of the velocity at which the tool is moving. The theoretical results from figure 9 show that for this diameter rolling will occur no matter which external contact force is applied. However, with the current setup it is rather difficult to obtain a good repeatability with the rolling strategy: no force sensor has yet been integrated on the micro robot, so it is difficult to maintain the contact between the tool and object while rolling. A setup for performing the rolling strategy with force feedback is presented in [16]. No experiments on rolling from teflon to teflon or from silicon to teflon have been carried out yet.

4.3. Transfer by scraping

Figure 8(*b*) shows the principle of the transfer of a micro object from a tool to the substrate (or other tool) by scraping with the tool at the border of the substrate. Intuitively, one would say that it is more difficult to transfer an object by scraping from a high surface energy material to a low surface energy material than transferring in the other direction. The critical moment during this transfer is just before the release when the corner of the tool is touching the micro object as depicted in figure 11(*a*). If the adhesion force between the tool and the object is too large at this moment, the object will stay in contact

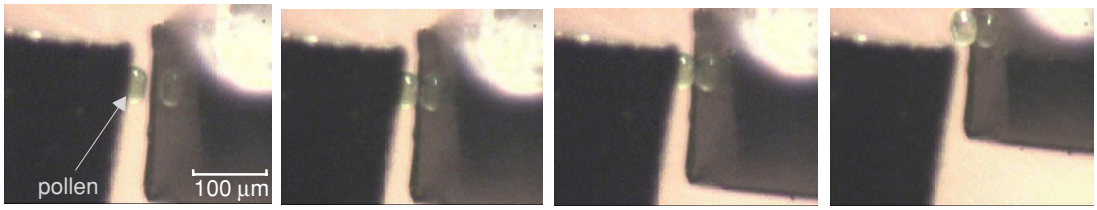

Figure 10. Transfer of a pollen micro sphere by rolling.

M An MPEG movie of this figure is available from stacks.iop.org/JMM/15/S259

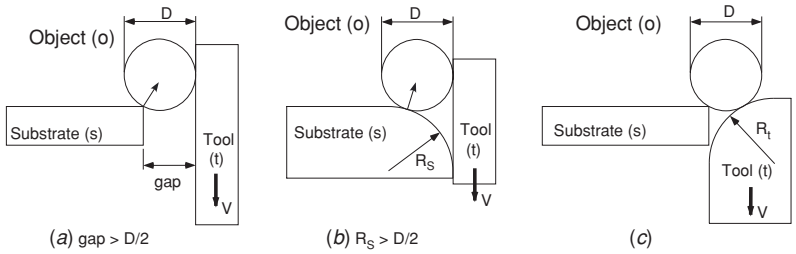

Figure 12. Influence of the gap and rounding radii on the behavior of the micro object during transfer by scraping.

with the tool and will roll around its corner (figure 11(*b*)). The gap between the tool and substrate should be smaller than the radius of the micro object, because if not, the object would be in contact with the corner of the substrate as shown in figure 12(*a*). If the rounding radius of the substrate corner is smaller than the radius of the micro object, this would reduce the adhesion force to the substrate, lowering the chance that the object will stay adhering to the substrate. Moreover, the reaction force between the object and substrate would have a horizontal component, which would tend to push the object over the corner of the tool (figure 11(*b*)). The same horizontal component of the reaction force between the object and substrate exists in the case of a substrate rounding radius R_s that is larger than the radius of the object (figure 12(*b*)). In fact, it is the sum of the gap and substrate rounding radius that should be smaller than the radius of the micro object to be handled. Also the rounding radius of the tool R_t should be as small as possible, because otherwise the adhesion force between the object and the tool at the critical moment would be increased, which would increase the chance of the object to roll over the corner of the tool (figure 12(*c*)). So it can be concluded that the gap between the tool and substrate and the rounding radii of the tool and substrate should be as small as possible.

Several microfabrication techniques exist that are capable of creating edges with a rounding radius smaller than 1 μm. The best way to minimize the gap between the tool and the substrate is to keep them always in contact. This is much easier than keeping the contact between the substrate and the object in the case of transfer by rolling as there is no danger of crushing the micro object. The contact between the tool and the substrate can be guaranteed with the proposed micro robotic setup without any additional force feedback by just pushing the tool against the substrate while doing the scraping motion. So, it can be concluded that neither the gap between the tool and substrate nor the rounding radii of the tool and substrate should pose any severe problems for the transfer by scraping of objects of a diameter down to $\varnothing$ 1 μm.

A complete model of the interacting forces on the critical moment would be quite complicated and is beyond the scope of this paper as the theory of the adhesion force between a sphere and a plane discussed in section 3 is not valid at the critical moment. However, it is easier to study the behavior of the object just before the critical moment when there is still a sphere–plane contact (as in figure 8(*b*)). If the object will roll just before the critical moment, there is a great chance that it will tend to roll around the corner of the tool during the critical moment. The equations presented below consider the situation of figure 8(*b*) in the case when the material of the tool and substrate are the same.

As the material of the substrate and tool is supposed to be the same, both adhesion forces are equal:

$$A = A_s = A_t. \tag{24}$$

On the assumption of a quasistatic process, the equilibrium equations for the object

$$f_s = N_t - A \tag{25}$$

$$f_t = N_s - A \tag{26}$$

$$R(f_t - f_s) = M_s + M_t \tag{27}$$

and for the tool

$$F_x = N_t - A = f_s \tag{28}$$

$$F_y = f_t \tag{29}$$

can be obtained.

Pure sliding without rolling between the object and the substrate is impossible as the tool is assumed to move in the Y direction. Sliding between the tool and the object occurs when the required friction force f_t exceeds its maximum value,

$$f_t = F_y > f_{t,max} = \mu N_t \tag{30}$$

or with equation (28),

$$F_y > \mu(A + f_s). \tag{31}$$

f_s is limited by the maximum friction force between the substrate and the object:

$$f_{s,max} = \mu N_s = \mu(A + F_y). \tag{32}$$

Hence, a sufficient condition for equation (31) is

$$F_y > \mu(A + f_{s,max}) = \mu(A + \mu(A + F_y)) \tag{33}$$

or

$$F_y > \frac{\mu}{1-\mu} A. \tag{34}$$

Rolling occurs when the moment generated by both friction forces f_s and f_t exceeds the sum of the two maximum rolling resistances $M_{t,max}$ and $M_{s,max}$:

$$R(f_t - f_s) > M_{t,max} + M_{s,max}. \tag{35}$$

The object can only roll over the tool if at the same time it is also sliding over the substrate. Consequently, f_s is equal to the maximum friction force $f_{s,max}$ as described in equation (32). Consequently, with equations (29) and (7) equation (35) becomes now

$$F_y > \frac{1}{1-\mu} \frac{c_r W}{R} (a_s + a_t) + \frac{\mu}{1-\mu} A. \tag{36}$$

Figure 13. Transfer of a pollen micro sphere by scraping.
M An MPEG movie of this figure is available from stacks.iop.org/JMM/15/S259

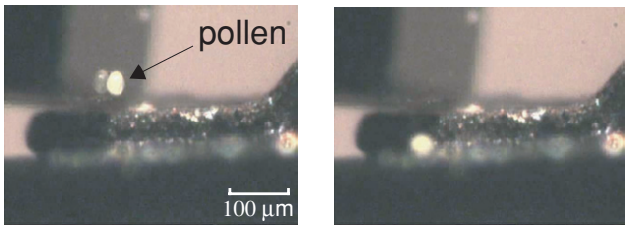

(*a*) (*b*)

Figure 14. Release of a pollen micro sphere by acceleration.
(*a*) Pollen adhering to tool. (*b*) Pollen has fallen on to the substrate.
M An MPEG movie of this figure is available from stacks.iop.org/JMM/15/S259

By comparison between equations (36) and (34) it can be easily concluded that the condition for rolling is more severe than the one for sliding between the tool and the object. Consequently, when increasing the force F_y, the maximum friction force will be reached before the maximum rolling resistance. When the object radius decreases, the difference between the limit for sliding and the limit for rolling will also increase, as the first term of equation (36) increases with decreasing R. So, it can be concluded that, whatever the object radius, the object will slide over the tool.

Figure 13 illustrates a transfer of a pollen micro sphere from one silicon tool to another by the scraping strategy. Experiments have shown that if the gap bewteen both tools is too big, the object still makes a rolling motion just at the end and rolls around the corner of the tool (figure (12(*a*)).

4.4. Transfer and release by applying high acceleration

As dimensions decrease adhesion forces become more important than gravitational forces. However, by applying a high acceleration (much higher than g), inertial forces can still become larger than the adhesion force. This effect can be used for the complete release of a micro object adhering to a tool [17]. The minimum acceleration to be applied can be calculated according to JKR theory as

$$a > \frac{A}{m} = \frac{\frac{3}{2}\pi W R}{\frac{4}{3}\pi R^3 \rho} = \frac{9}{8}\frac{W}{R^2 \rho}. \tag{37}$$

For a $\varnothing 40\,\mu$m pollen sphere (effective density $\rho = 549\ \mathrm{kg\ m^{-3}}$), the required acceleration is $a = 2.3 \times 10^6\ \mathrm{m\ s^{-2}}$.

It is quite difficult to calculate exactly what is the maximum acceleration that can be applied by the piezoelectric actuator on the robot, but the estimation calculated below gives an idea of the order of magnitude. The micro object is adhering to a piece of silicon which is mounted on top of the piezoelectric actuator. Contrary to the setup presented in [17], the silicon does not form a cantilever, but is completely supported by the piezoelectric actuator. The resonance frequency of only the piezoelectric actuator should be calculated by considering a lumped parameter model, but it can also be approximated by considering a mechanical model with an effective mass that is one third of the mass of the piezoelectric actuator. Hence, the resonance frequency of the mechanical system consisting of the piezoelectric actuator and the piece of silicon can be approximated by considering a mass–spring model with an effective mass that is equal to the mass of the piece of silicon plus one third of the mass of the piezoelectric actuator,

$$f_\mathrm{n} = \frac{1}{2\pi}\omega_\mathrm{n} \simeq \frac{1}{2\pi}\sqrt{\frac{k}{m_\mathrm{eff}}} = \frac{1}{2\pi}\sqrt{\frac{k}{m_\mathrm{Si} + \frac{m_\mathrm{piezo}}{3}}} = 2.08\ \mathrm{MHz} \tag{38}$$

for Young's modulus $E = 52.63$ GPa, a density $\rho_\mathrm{piezo} = 7800\ \mathrm{kg\ m^{-3}}$, $\rho_\mathrm{Si} = 2330\ \mathrm{kg\ m^{-3}}$ and an actuator and silicon thickness of 0.25 mm. The piezoelectric material that has been used (PIC 151 from Physik Instrumente) has a mechanical Q of 120, which means that a fraction $1/120 = 0.0083$ of the mechanical input energy is converted to internal heating. For a mass–spring system with such a low damping, the step

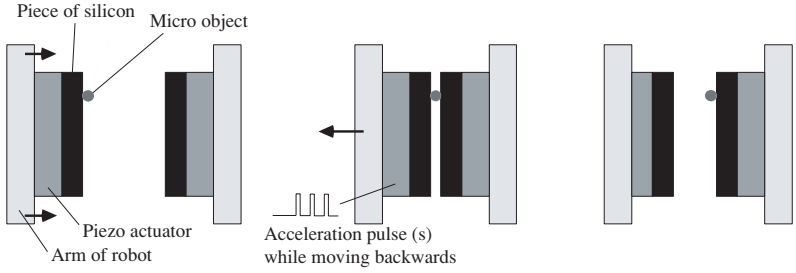

Figure 15. Bidirectional transfer of a micro object from one tool to another by acceleration.

response resembles very much a sinusoidal vibration with the step height as amplitude. Hence, the maximum acceleration can be approximated by

$$a_{\max} = \Delta z \omega_n^2 = 5.81 \times 10^6 \text{ ms}^{-2} \quad (39)$$

for a step height $\Delta z = 34$ nm, which is obtained from a voltage pulse of 75 V that is applied to a piezoelectric actuator with a charge constant of $d_{33} = 450 \times 10^{-12}$ m V^{-1}. This maximum acceleration is of the same order of magnitude as the acceleration required for releasing a micro object with a diameter of $\varnothing 40\,\mu$m as calculated from equation (37). This would mean that the release of a $\varnothing 40\,\mu$m object is possible, but when decreasing the diameter of the micro object, the limits of the system will be reached quickly.

Figure 14 shows the release of a $\varnothing 40\,\mu$m pollen micro sphere after which it falls on to the substrate. The experiments show that the pollen sphere can be released in most cases, but sometimes the object seems to adhere strongly to the surface and the acceleration is no longer sufficient to release it. These experimental results confirm that we are close to the limits of the system. A more systematic study of the potential of this strategy is beyond the scope of this paper and can be found in [17].

The acceleration strategy has also been used for the bidirectional transfer of a micro object from one tool to another and back as illustrated in figure 15.

5. Conclusion

In this paper, the functionality and the great flexibility of the micro robots developed by EPFL have been proven by carrying out several experiments concerning the manipulation by adhesion of micro spheres. Four strategies for grasping, releasing and transferring a micro object from one tool to another have been discussed. All strategies have been experimentally verified by the manipulation of pollen micro spheres with a diameter of some tens of micrometers without the integration of any advanced position control or force feedback. Grasping from a substrate with low adhesion is reliable and very simple, but it only works in one direction. The rolling strategy is bidirectional, but with the current setup it is difficult to reach good repeatability, as no force sensor has been integrated yet on the robot. The scraping strategy is a very reliable transfer strategy that can be easily realized without any extra sensors. Release by acceleration has also proven to be quite reliable, but with the current setup it will be difficult to release pollen spheres of a diameter much smaller than $\varnothing 40\,\mu$m. The acceleration strategy is the only strategy that can be used to release an object from the tool and drop it on a substrate of any shape and material.

Future work will focus on an in-depth study of the theoretical aspects of the proposed strategies and on the further optimization of the micro manipulation setup.

Acknowledgments

This research was supported by the Swiss Office on Education and Science (OFES no 01.0365, EU project no IST-2001-33567). The authors acknowledge partial financial support from the 'LEA-Microtechnique-European Associated Laboratory for Microtechnology'.

References

[1] Sulzmann A, Breguet J M, Carlier J and Jacot J 1996 Virtual reality and high accurate vision feedback as key information for micro robot telemanipulation *Microrobotics: Components and Applications, Proc. SPIE* **2906** 38–57

[2] Fatikow S, Seyfried J, Fahlbusch S, Buerkle A and Schmoeckel F 2000 *J. Intell. Robot. Syst.* **27** 135–69

[3] Martel S, Sherwood M, Helm C, Garcia de Quevedo W, Fofonoff T, Dyer R, Bevilacqua J, Kaufman J, Roushdy O and Hunter I 2001 Three-legged wireless miniature robots for mass-scale operations at the sub-atomic scale *Proc. IEEE Int. Conf. on Robotics and Automation (Seoul)* vol 4 pp 3423–8

[4] Caprari G, Estier T and Siegwart R 2001 *J. Micromechatron.* **1** 177–90

[5] Aoyama H, Fuchiwaki O and Misaki D 2004 Piezo based micro robots system for precise micro bio and chemical applications *Int. Conf. on New Actuators (Bremen)* pp 164–7

[6] Estaña R and Woern H 2003 Moire-based positioning system for microrobots *Proc. Optical Measurement Systems for Industrial Inspection III (München), Proc. SPIE* **5144** pp 431–42

[7] Driesen W, Bergander A, Varidel T and Breguet J-M 2003 Energy consumption of piezoelectric actuators for inertial drives *Proc. IEEE Int. Symp. on Micromechatronics and Human Science (Nagoya)* pp 51–8

[8] Breguet J-M and Clavel R 1998 Stick and slip actuators: design, control, performances and applications *Proc. IEEE Int. Symp. on Micromechatronics and Human Science (Nagoya)* pp 89–95

[9] Varidel T, Driesen W, Bergander A and Breguet J-M 2004 High resolution miniature rotary microactuator *Int. Conf. on New Actuators (Bremen)* pp 517–20

[10] Johnson K L, Kendall K and Roberts A D 1971 *Proc. R. Soc.* A **324** 301–13

[11] Derjaguin B V, Muller V M and Toporov Y P 1975 *J. Colloid Interface Sci.* **53** 314–26

[12] Maugis D 1992 *J. Colloid Interface Sci.* **150** 243–69

[13] Carpick R W, Ogletree D F and Salmeron M 1999 *J. Colloid Interface Sci.* **221** 395–400

[14] Heim L-O, Blum J, Preuss M and Butt H-J 1999 *Phys. Rev. Lett.* **83** 3328–31

[15] Saito S, Miyazaki H T, Sato T and Takahashi K 2002 *J. Appl. Phys.* **92** 5140–9

[16] Dionnet R, Haliyo D S and Régnier S 2004 *IEEE Proc. Int. Conf. on Robotics and Automation (New Orleans)* vol 5 pp 5019–24

[17] Haliyo D S, Rollot Y and Régnier S 2002 Manipulation of micro-objects using adhesion forces and dynamical effects *IEEE Proc. Int. Conf. on Robotics and Automation (Washington, DC)* vol 2 pp 1949–54